

Boundary between noise and information applied to filtering neural network weight matrices

Max Staats,* Matthias Thamm,* and Bernd Rosenow

Institut für Theoretische Physik, Universität Leipzig, Brüderstrasse 16, 04103 Leipzig, Germany

(Dated: June 9, 2022)

Deep neural networks have been successfully applied to a broad range of problems where over-parametrization yields weight matrices which are partially random. A comparison of weight matrix singular vectors to the Porter-Thomas distribution suggests that there is a boundary between randomness and learned information in the singular value spectrum. Inspired by this finding, we introduce an algorithm for noise filtering, which both removes small singular values and reduces the magnitude of large singular values to counteract the effect of level repulsion between the noise and the information part of the spectrum. For networks trained in the presence of label noise, we indeed find that the generalization performance improves significantly due to noise filtering.

Introduction: In recent years, deep neural networks (DNNs) have proven to be powerful tools for solving a wide range of problems [1–5], including a large number of applications in physics [6–16]. Many of these networks are highly over-parametrized [17–23] and not only generalize well beyond the training data set, but also have the capacity to memorize large amounts of completely random data [24, 25]. However, if the training data set contains label noise, i.e. mislabeled examples (which is almost inevitable for realistic, large datasets [26]), overfitting the training data can significantly decrease the generalization performance [27].

In several studies, random matrix theory has been successfully applied to the analysis of neural networks [28–36]. Since weights of neural network are usually initialized randomly, learned information after training can be interpreted as deviations from random matrix theory (RMT) predictions, and it has been shown that even state of the art DNNs have weights that follow RMT predictions [34, 36]. The singular value distribution can be decomposed into a bulk and a tail region, where the random bulk can be fitted with a Marchenko-Pastur distribution appropriate for random matrices. The theory of the Gaussian orthogonal ensemble accurately describes the level spacing and the level number variance of the bulk of the singular values in DNN weight matrices, and most of the singular vectors follow the Porter-Thomas distribution. Deviations from RMT only occur for some large singular values and corresponding vectors [34, 36], explaining the success of low-rank approximations [37–43].

In this letter we study weight matrices for a variety of DNN models and architectures trained with and without label noise. We quantify how well singular vector components follow the Porter-Thomas distribution by applying a Kolmogorov-Smirnov test which takes into account the normalization of vectors, and find that there is a boundary between noise and information: singular vectors with

small singular values agree with the RMT prediction, while vectors with large singular values significantly deviate. We confirm this finding by setting singular values to zero, starting from the smallest one, and evaluate the dependence of the training and test accuracy on the percentage of removed singular values. We find that small singular values and the associated vectors indeed do not encode information. When training networks in the presence of label noise, more singular values are needed for a good training performance as compared to the pristine data set, indicating that label noise is encoded predominantly in intermediate singular values. Motivated by these results we suggest an algorithm for noise filtering of neural network weight matrices: we filter the spectra from noise by (i) removing small and intermediate singular values and (ii) by reverting the shift of large singular values due to level repulsion with the noisy bulk. We find that this algorithm improves the test accuracy of DNNs trained with label noise by up to 6 %.

Setup: We train several DNNs on the CIFAR-10 dataset [44] containing $N = 50000$ training images $\mathbf{x}^{(k)}$ sorted into ten different classes, where the corresponding labels $\mathbf{y}^{(k)}$ are vectors with an entry of one at the position of the class and zeros otherwise. For training with label noise, we randomly shuffle a certain percentage of the labels to force the networks to learn this noise in addition to the underlying rule. In a feed-forward DNN, the l -th layer with n_l neurons is described by an $n_{l-1} \times n_l$ weight matrix \mathbf{W}_l , a bias vector \mathbf{b}_l of length n_l , and an activation function f_l such that an input image \mathbf{x} activates the neurons in the input layer according to $\mathbf{a}_0 = \mathbf{x}$ and the activations are then passed through the network via

$$\mathbf{a}_l = f_l(\mathbf{W}_l \mathbf{a}_{l-1} + \mathbf{b}_l) . \quad (1)$$

The largest entry in the activation of the output layer \mathbf{a}_{out} then determines the network’s prediction for the class of the input \mathbf{x} . For initialization of the networks, we choose zeros for the biases, draw random weights from a Glorot uniform distribution [45], and choose ReLU activations $f_l(\xi_i) = \max(\xi_i, 0)$ for hidden layers and softmax $f_{\text{out}}(\xi_i) = \exp(\xi_i) / \sum_j \exp(\xi_j)$ for the output layer. Dur-

* These authors contributed equally to this work.

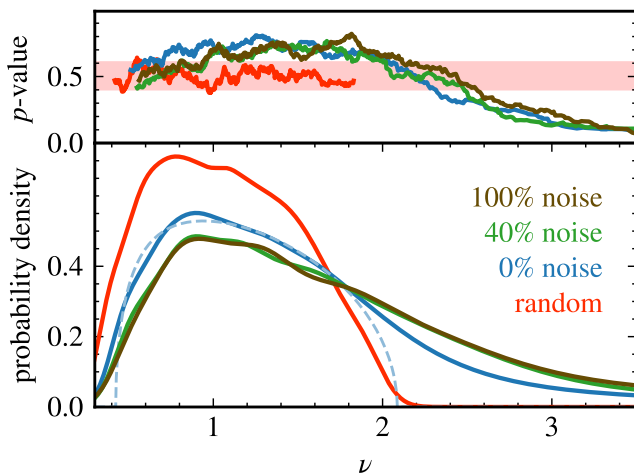


Figure 1. Analysis of singular values ν and vectors V of the first hidden layer weight matrix for the MLP1024 network trained with various amounts of label noise: 0% (blue), 40% (green), and 100% (brown). For reference, we show results for randomly initialized weights in red. The upper panel shows the randomness of singular vectors via the p -value of Kolmogorov-Smirnov tests against a Thomas-Porter distribution, averaged over neighboring singular values with a window size of 15; the light red stripe describes the 2σ region around the mean for random vectors. The lower panel depicts the corresponding singular value spectra obtained via Gaussian broadening with a window size of 15 (solid lines). The dashed line shows the fit of a Marchenko-Pastur distribution to the spectrum for 0% label noise.

ing training, the network is presented the image-label pairs in mini-batches of size 32 while gradient descent is used to adjust weights and biases such that the loss function

$$\ell(\mathbf{W}, \mathbf{b}) = -\frac{1}{N} \sum_{k=1}^N \mathbf{a}_{\text{out}}^{(k)} \cdot \ln \mathbf{y}^{(k)} \quad (2)$$

is minimized, i.e. such that the network’s predictions agree with the labels (details of training parameters in [46]). We train two kinds of architectures: (i) fully connected networks with three hidden layers, denoted as MLP1024, with layer sizes [in, 1024, 512, 512, out], and (ii) modern convolutional neural networks (CNNs), called miniAlexNet [25], consisting of two convolutional layers followed by max-pooling, batch normalization, and fully connected layers with regularization. To show that our results are generic, we additionally consider the two large networks alexnet [47] and vgg19 [21] pretrained on the imagenet dataset [47] with 1000 classes. We compute the singular value decompositions $\mathbf{W} = \mathbf{U} \text{diag}(\nu) \mathbf{V}$ with orthogonal matrices \mathbf{U} , \mathbf{V} containing the singular vectors, and non-negative singular values ν for the dense fully connected layers described above. For convolutional layers in CNNs, we first need to reshape the convolutional layer weight tensors to a rectangular shape and then perform

the singular value decomposition described above [46].

Boundary between noise and information: For a random weight matrix in the limit of large matrix dimension, the components of an m -dimensional singular vectors follow a Porter-Thomas distribution, i.e. a normal distribution with zero mean and standard deviation $1/\sqrt{m}$. For the finite dimensional weight matrices we study here, the fact that singular vectors are normalized introduces correlations between the singular vector entries. To account for these correlations, we compute the Kolmogorov-Smirnov test statistic with Monte-Carlo methods [46] and apply the test to the empirical distribution of the singular vectors V of trained networks. The resulting p -values, $0 \leq p < 1$, indicate the likelihood of the sample to be from the test distribution. In order to reduce the amount of fluctuations in the p -values, we average over a window of size 15 centered around a given singular vector. The averaged p -values of a random control fluctuate around 0.5 with a standard deviation of $\sigma = 0.05$.

For the MLP1024 architecture in the absence of label noise, we find that the averaged p -values drop below two standard deviations of the random control for singular values larger than 2.3, corresponding to 14.3 percent of deviating singular values (blue solid line in the upper panel of Fig. 1), indicating that information may be contained in these singular vectors. For vectors corresponding to small singular values, the p -values lie within or even above the 2σ region (this latter deviation is due to the requirement of orthogonality with vectors belonging to large singular values [46]). Interestingly, the p -values in the regime of large singular values barely increase in the presence of 40% label noise. Only for completely random labels (100% label noise) the p -values are somewhat increased, which is plausible since random labels should result in more random singular vectors.

As a second approach [34, 36], we directly compare the empirical singular values to a Marchenko-Pastur distribution [48] valid for random matrices. The bulk of small singular values can be fitted with a Marchenko-Pastur distribution (lower panel), which describes the spectrum of randomly initialized weight matrices (dashed line, details in [46]). The upper end of such a fit is for singular values $\lambda \approx 2$, in agreement with the value 2.3 found above for which the p -value is outside the 2σ -interval of the random control.

To verify the hypothesis that system specific information is stored in singular vectors corresponding to large singular values, we set singular values to zero, starting from the smallest one, and monitor the training and test accuracy of the networks (Fig. 2). The training accuracy (blue lines, MLP1024 in panel (a), miniAlexNet in panel (b)) indeed shows that learned information is stored only in the largest singular values and corresponding vectors. Label noise is learned differently from the rule and mainly stored in intermediate singular values such that the train-

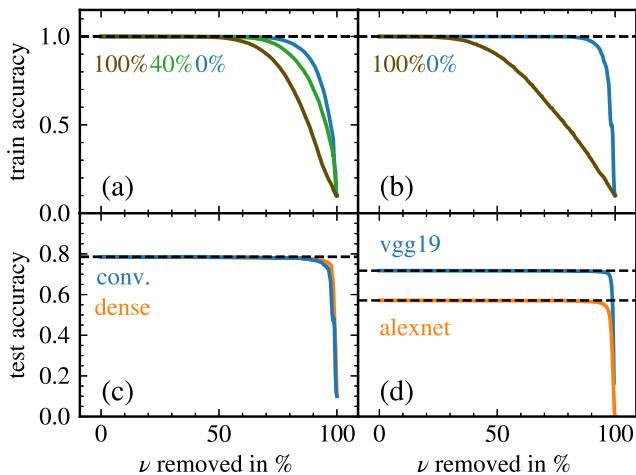


Figure 2. Information-noise boundary, demonstrated by setting a given percentage of the singular values to zero. (a) Training accuracy for the MLP1024 network trained with various amounts of label noise (0% blue, 40% green, and 100% brown). (b) Training accuracy for setting singular values from the second convolutional layer of miniAlexNet trained with 0% label noise (blue) and 100% label noise (brown) to zero. (c) Test accuracy for miniAlexNet trained without label noise for setting singular values to zero in the first dense layer (orange) and the second convolutional layer (blue). (d) Test accuracy for the pre-trained networks vgg19 [21] (third dense layer, blue) and alexnet [47] (second dense layer, orange). In all cases, relevant information is stored in the largest singular values and corresponding vectors only. In presence of label noise larger parts of the spectrum are needed to store the noise.

ing accuracy drops significantly earlier in the case of label noise (40% noise: green line, 100% noise: brown lines; other amounts (not shown) interpolate). This behavior is even more pronounced for a convolutional layer of miniAlexNet (Fig. 2b), where the training accuracy drops sharply when removing more than 30% of singular values, compared to a threshold of about 90% for the pristine training data.

When considering the dependence of the test accuracy on the removal of singular values (Fig. 2b and 2c) it becomes apparent that generalization is solely due to the largest singular values and corresponding vectors. This is also valid for the large state of the art networks alexnet (orange) and vgg19 (blue) in Fig. 2d. The observation that neural networks use only a small fraction of large singular values and vectors to learn the underlying rule sheds some light on the puzzle why neural networks generalize well even though their capacity allows them to memorize random labels with ease, since larger singular values and vectors store the rule, and intermediate ones can be utilized for memorizing random labels.

Noise filtering of weights: We next study how the generalization performance of DNNs trained with label noise depends on the removal of singular values. In Fig. 3

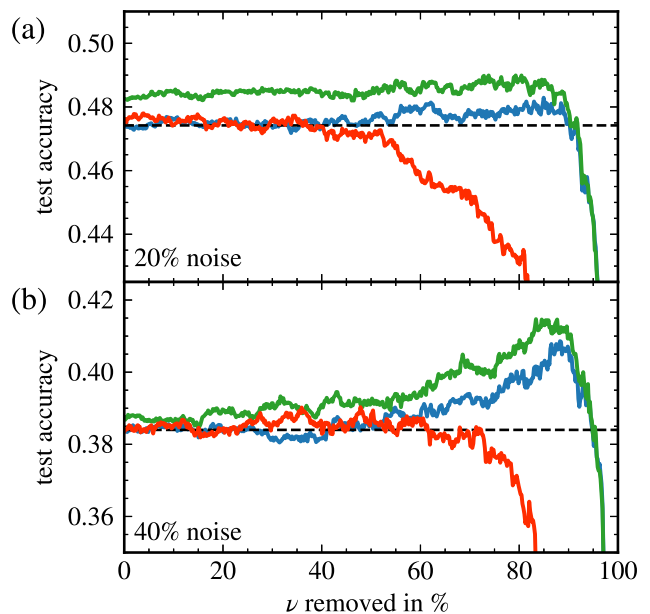


Figure 3. Dependence of the test accuracy on the removal and shifting of singular values from the second hidden layer weights of MLP1024 networks trained in the presence of label noise: upon setting singular values to zero (blue) and when additionally shifting them according to Eq. (3) (green) we observe a significant improvement in performance. For training with overfitting (red) no improvement is observed, indicating that information and noise are mixed in the spectrum.

we show the impact on the test accuracy of setting singular values to zero (blue lines) in all hidden layers of MLP1024 networks trained with 20% label noise (upper panel) and 40% label noise (lower panel). In the latter case, the generalization accuracy improves by up to 2.5% when removing about 90% of singular values.

In addition, we train another set of MLP1024 networks with severe overfitting, i.e. we train for much longer than necessary to achieve 100% training accuracy, with a slower learning rate schedule [46]. This causes an earlier drop of the test accuracy when removing singular values (red line, Fig. 3), without any noticeable improvements before the drop. We interpret this behavior as a mixing between information and noise in the spectra such that no clear boundary between these regimes exists anymore.

Level repulsion in random matrices can lead to an upward shift of large singular values in the presence of a random bulk of smaller singular values. Such a shift of eigenvalues was discussed in [49] for the case of a linear network, and is also known to exist in empirical covariance matrices, e.g. between returns of a stock portfolio [50, 51]. For the latter case, estimators have been developed which compensate for this singular value shift [52, 53]. Here, we suggest to model the contribution of the weights' noisy bulk W_{noise} to the low rank part W_0 containing the information in an additive way, such that the weight matrix

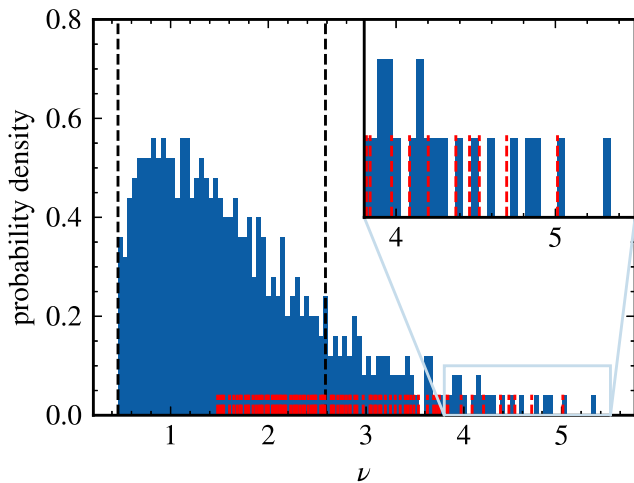


Figure 4. Shifting of singular values: histogram of singular values for the first hidden layer weight matrix of the MLP1024 network (blue) trained with 40% label noise, with boundaries of the Marchenko-Pastur region (dashed black lines). The dashed red lines show the locations of shifted singular values according to Eq. (3), and the inset zooms into the tail region.

after training is given by $W = W_0 + W_{\text{noise}}$. The upwards shift of large singular values due to level repulsion can then be explicitly computed [49, 54] in the limit where the dimensions of the $n_{l-1} \times n_l$ weight matrix tend to infinity with a fixed ratio $q = n_l/n_{l-1} \leq 1$. Under the assumption of i.i.d distributed elements of W_{noise} with standard deviation σ , the singular values ν of W can be shifted back to recover the unperturbed singular values ν_0 of W_0 via

$$\frac{\nu_0}{\sigma} = \sqrt{\left(\frac{\nu}{\sigma}\right)^2 - q - 1 + \sqrt{\left(\left(\frac{\nu}{\sigma}\right)^2 - q - 1\right)^2 - 4q}}, \quad (3)$$

where the standard deviation of the noise term σ is obtained from a Marchenko-Pastur fit to the spectrum (for details see [46]). The effect of such a transformation is shown in Fig. 4: While large values are shifted by a relatively small amount as seen in the inset, there are several singular values that get pushed far into the MP region. When applying a shift of singular values originally outside the Marchenko-Pastur region together with the removal of singular values, we use the following algorithm: we i) rank order the singular values, then ii) shift the large singular values while keeping their rank within the spectrum unchanged, and then iii) remove singular values from small to large according to their rank. The green lines in Fig. 3 describe the dependence of test accuracy on both shifting and removing singular values in the first two hidden layers of MLP1024 networks trained with 20% label noise (upper panel) and 40% label noise (lower panel), respectively. We find significant improve-

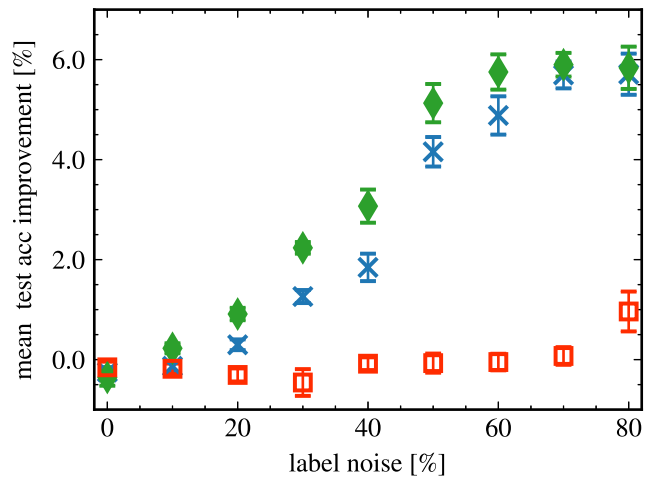


Figure 5. Average improvement of the test accuracy when removing singular values (blue, red) from all layers and when additionally shifting singular values (green) of the first two layers in MLP1024 networks, with results for both the learning rate schedule (blue crosses, green diamonds) and an overfitting schedule (red squares). We observe that the average improvements increase with increasing amount of label noise, with an enhanced improvement for additionally shifting singular values. There are no improvements for networks trained with overfitting.

ments of the generalization accuracy using a combination of shifting and removing singular values (similar for the convolutional layer of miniAlexNet [46]) as compared to only removing them.

To study the typical improvement in test accuracy when noise filtering DNN weight matrices, we train MLP1024 networks initialized using ten different seeds on the 50000 CIFAR-10 training images for both training schedules at amounts of label noise varying between 0% and 80%. We split the remaining 10000 images from the dataset into a validation set of 2000 images and a test set of 8000 images. Using the validation data we determine the optimum amount of singular values to be removed for all layers, except for the output ones with only ten singular values. We optimize by moving from the last layer to the first one, while always fixing the previously filtered weights when optimizing the next layer. We determine the amount of singular values to be removed in each layer from the maximum of the validation accuracy, when consecutively setting singular values to zero, starting with the smallest one. In the cases where we additionally shift singular values, we compare the accuracy of both shifting and removing an optimal amount of singular values in a given layer layer with the accuracy of only removing singular values, and then choose the algorithm with the better validation accuracy. In this process, we do not optimize over the amount of singular values which are shifted, but instead determine the smallest singular value to be shifted by the upper boundary of

a Marchenko-Pastur fit to the bulk part of the spectrum as described above.

In Fig. 5 one sees that for networks trained with the regular schedule an average increase of roughly 1% already in the case of 20% label noise is achieved by a combination of shifting and removing (green symbols). Increasing the label noise further we find significant improvements of several percent. However, for the overfitted networks (red symbols) no improvements of the test accuracy are obtained when filtering the singular values. For the pretrained network vgg19 we find that shifting singular values of the last layers can decrease the test accuracy, while small improvements of 0.3% percent are possible on the validation data set when shifting and removing from the first two layers. However, no improvements can be observed on the test set. Here, we randomly drew 2000 images from the original imagenet test set as a validation set and another 8000 as our new test set such that the two sets are disjoint.

Conclusions. By comparing singular vectors to the Porter-Thomas distribution and singular values to a Marchenko-Pastur law, we argue that weight matrices of DNNs exhibit a boundary between noise and information in their spectra. We substantiate this concept by systematically setting singular values to zero while monitoring the impact on the training and test accuracy. It turns out that (i) small singular values do not contribute to either training or test performance, (ii) large singular values encode the underlying rule, and (iii) intermediate singular values are important for the training accuracy when learning images with label noise, even though they correspond to random singular vectors. We suggest a filtering algorithm combining the removal of small singular values with the downward shift of large ones and find that it increases the generalization performance significantly in the presence of label noise. As label noise can be inherent in datasets where label annotation is difficult, we believe that filtering of weight matrices could be useful for improving the performance of DNNs in such situations.

Acknowledgments. This work has been funded by the Deutsche Forschungsgemeinschaft (DFG) under Grants No. RO 2247/11-1 and No. 406116891 within the Research Training Group RTG 2522/1.

* These authors contributed equally to this work.

- [1] Y. LeCun, Y. Bengio, and G. Hinton, Deep learning, Nature **521**, 436 (2015).
- [2] I. Goodfellow, Y. Bengio, and A. Courville, *Deep learning* (MIT press, 2016).
- [3] G. Carleo, I. Cirac, K. Cranmer, L. Daudet, M. Schuld, N. Tishby, L. Vogt-Maranto, and L. Zdeborová, Machine learning and the physical sciences, Reviews of Modern Physics **91**, 045002 (2019).
- [4] D. Silver, J. Schrittwieser, K. Simonyan, I. Antonoglou, A. Huang, A. Guez, T. Hubert, L. Baker, M. Lai, A. Bolton, *et al.*, Mastering the game of go without human knowledge, Nature **550**, 354 (2017).
- [5] Y. Bahri, J. Kadmon, J. Pennington, S. S. Schoenholz, J. Sohl-Dickstein, and S. Ganguli, Statistical mechanics of deep learning, Annual Review of Condensed Matter Physics **11**, 501 (2020).
- [6] J. Carrasquilla and R. G. Melko, Machine learning phases of matter, Nature Physics **13**, 431 (2017).
- [7] E. P. L. van Nieuwenburg, Y.-H. Liu, and S. D. Huber, Learning phase transitions by confusion, Nature Physics **13**, 435 (2017).
- [8] K. Ch'ng, J. Carrasquilla, R. G. Melko, and E. Khatami, Machine learning phases of strongly correlated fermions, Physical Review X **7**, 031038 (2017).
- [9] P. Broecker, J. Carrasquilla, R. G. Melko, and S. Trebst, Machine learning quantum phases of matter beyond the fermion sign problem, Scientific reports **7**, 1 (2017).
- [10] P. Huembeli, A. Dauphin, and P. Wittek, Identifying quantum phase transitions with adversarial neural networks, Physical Review B **97**, 134109 (2018).
- [11] M. Koch-Janusz and Z. Ringel, Mutual information, neural networks and the renormalization group, Nature Physics **14**, 578 (2018).
- [12] C. Lee, J. Kim, D. Babcock, and R. Goodman, Application of neural networks to turbulence control for drag reduction, Physics of Fluids **9**, 1740 (1997).
- [13] X. Jin, S. Cai, H. Li, and G. E. Karniadakis, Nsfnets (navier-stokes flow nets): Physics-informed neural networks for the incompressible navier-stokes equations, Journal of Computational Physics **426**, 109951 (2021).
- [14] Z. Chen, J. Gao, W. Wang, and Z. Yan, Physics-informed generative neural network: an application to troposphere temperature prediction, Environmental Research Letters **16**, 065003 (2021).
- [15] J. Duarte, S. Han, P. Harris, S. Jindariani, E. Kreinar, B. Kreis, J. Ngadiuba, M. Pierini, R. Rivera, N. Tran, *et al.*, Fast inference of deep neural networks in fpgas for particle physics, Journal of Instrumentation **13** (07), P07027.
- [16] D. Guest, K. Cranmer, and D. Whiteson, Deep learning and its application to lhc physics, Annual Review of Nuclear and Particle Science **68**, 161 (2018).
- [17] I. J. Goodfellow, O. Vinyals, and A. M. Saxe, Qualitatively characterizing neural network optimization problems, preprint arXiv:1412.6544 (2014).
- [18] D. Soudry and E. Hoffer, Exponentially vanishing sub-optimal local minima in multilayer neural networks, preprint arXiv:1702.05777 (2017).
- [19] Siyuan Ma, Raef Bassily, and Mikhail Belkin, The Power of Interpolation: Understanding the Effectiveness of SGD in Modern Over-parametrized Learning, International Conference on Machine Learning , 3325 (2018).
- [20] K. Kawaguchi, L. P. Kaelbling, and Y. Bengio, Generalization in deep learning, arXiv preprint arXiv:1710.05468 (2017).
- [21] K. Simonyan and A. Zisserman, Very Deep Convolutional Networks for Large-Scale Image Recognition, preprint arXiv:1409.1556 (2014).
- [22] X. Zhai, A. Kolesnikov, N. Houlsby, and L. Beyer, Scaling Vision Transformers, preprint arXiv:2106.04560 (2021).

- [23] O. Cohen, O. Malka, and Z. Ringel, Learning curves for overparametrized deep neural networks: A field theory perspective, *Physical Review Research* **3**, 023034 (2021).
- [24] J. Lever, M. Krzywinski, and N. Altman, Points of significance: model selection and overfitting, *Nature methods* **13**, 703 (2016).
- [25] C. Zhang, S. Bengio, M. Hardt, B. Recht, and O. Vinyals, Understanding deep learning (still) requires rethinking generalization, *Communications of the ACM* **64**, 107 (2021).
- [26] B. Frénay and M. Verleysen, Classification in the presence of label noise: a survey, *IEEE transactions on neural networks and learning systems* **25**, 845 (2013).
- [27] S. Liu, Z. Zhu, Q. Qu, and C. You, Robust training under label noise by over-parameterization, preprint arXiv:2202.14026 (2022).
- [28] C. Louart, Z. Liao, and R. Couillet, A random matrix approach to neural networks, *The Annals of Applied Probability* **28**, 1190 (2018).
- [29] J. Pennington and P. Worah, Nonlinear random matrix theory for deep learning, *Journal of Statistical Mechanics: Theory and Experiment* **2019**, 124005 (2019).
- [30] A. K. Lampinen and S. Ganguli, An analytic theory of generalization dynamics and transfer learning in deep linear networks, preprint arXiv:1809.10374 (2018), arXiv:1809.10374 [stat.ML].
- [31] J. Pennington, S. Schoenholz, and S. Ganguli, The emergence of spectral universality in deep networks, in *Proceedings of the Twenty-First International Conference on Artificial Intelligence and Statistics*, Proceedings of Machine Learning Research, Vol. 84, edited by A. Storkey and F. Perez-Cruz (PMLR, 2018) pp. 1924–1932.
- [32] N. P. Baskerville, D. Granzol, and J. P. Keating, Applicability of Random Matrix Theory in Deep Learning, preprint arXiv:2102.06740.
- [33] D. Granzol, Beyond random matrix theory for deep networks, preprint arXiv:2006.07721 (2020).
- [34] C. H. Martin and M. W. Mahoney, Implicit self-regularization in deep neural networks: Evidence from random matrix theory and implications for learning, *Journal of Machine Learning Research* **22**, 1 (2021).
- [35] C. H. Martin, T. S. Peng, and M. W. Mahoney, Predicting trends in the quality of state-of-the-art neural networks without access to training or testing data, *Nature Communications* **12**, 4122 (2021).
- [36] M. Thamm, M. Staats, and B. Rosenow, Random matrix analysis of deep neural network weight matrices, preprint arXiv:2203.14661 (2022).
- [37] J. Xue, J. Li, and Y. Gong, Restructuring of deep neural network acoustic models with singular value decomposition., in *Interspeech* (2013) pp. 2365–2369.
- [38] C. Li and C. Shi, Constrained optimization based low-rank approximation of deep neural networks, in *Proceedings of the European Conference on Computer Vision (ECCV)* (2018) pp. 732–747.
- [39] H. Kim, M. U. K. Khan, and C.-M. Kyung, Efficient neural network compression, in *Proceedings of the IEEE/CVF Conference on Computer Vision and Pattern Recognition* (2019) pp. 12569–12577.
- [40] L. Liebenwein, A. Maalouf, O. Gal, D. Feldman, and D. Rus, Compressing neural networks: Towards determining the optimal layer-wise decomposition, preprint arXiv:2107.11442 (2021).
- [41] J. M. Alvarez and M. Salzmann, Compression-aware training of deep networks, *Advances in neural information processing systems* **30**, 856 (2017).
- [42] Y. Xu, Y. Li, S. Zhang, W. Wen, B. Wang, W. Dai, Y. Qi, Y. Chen, W. Lin, and H. Xiong, Trained rank pruning for efficient deep neural networks, in *2019 Fifth Workshop on Energy Efficient Machine Learning and Cognitive Computing-NeurIPS Edition (EMC2-NIPS)* (IEEE, 2019) pp. 14–17.
- [43] Y. Idelbayev and M. A. Carreira-Perpinán, Low-rank compression of neural nets: Learning the rank of each layer, in *Proceedings of the IEEE/CVF Conference on Computer Vision and Pattern Recognition* (2020) pp. 8049–8059.
- [44] A. Krizhevsky, G. Hinton, *et al.*, Learning multiple layers of features from tiny images, *Tech Report* (2009).
- [45] Xavier Glorot and Yoshua Bengio, Understanding the difficulty of training deep feedforward neural networks, *Proceedings of the Thirteenth International Conference on Artificial Intelligence and Statistics* , 249 (2010).
- [46] See supplemental material.
- [47] A. Krizhevsky, I. Sutskever, and G. E. Hinton, ImageNet classification with deep convolutional neural networks, *Communications of the ACM* **60**, 84 (2017).
- [48] V. A. Marčenko and L. A. Pastur, Distribution of eigenvalues for some sets of random matrices, *Mathematics of the USSR-Sbornik* **1**, 457 (1967).
- [49] A. K. Lampinen and S. Ganguli, An analytic theory of generalization dynamics and transfer learning in deep linear networks, preprint arXiv:1809.10374 (2018).
- [50] L. Laloux, P. Cizeau, J.-P. Bouchaud, and M. Potters, Noise Dressing of Financial Correlation Matrices, *Physical Review Letters* **83**, 1467 (1999).
- [51] V. Plerou, P. Gopikrishnan, B. Rosenow, L. A. N. Amaral, and H. E. Stanley, Universal and nonuniversal properties of cross correlations in financial time series, *Physical Review Letters* **83**, 1471 (1999).
- [52] J. Bun, J.-P. Bouchaud, and M. Potters, Cleaning large correlation matrices: Tools from random matrix theory, *Physics Reports* **666**, 1 (2017).
- [53] R. Schäfer, N. F. Nilsson, and T. Guhr, Power mapping with dynamical adjustment for improved portfolio optimization, *Quantitative Finance* **10**, 107 (2010), <https://doi.org/10.1080/14697680902748498>.
- [54] F. Benaych-Georges and R. R. Nadakuditi, The singular values and vectors of low rank perturbations of large rectangular random matrices, *Journal of Multivariate Analysis* **111**, 120 (2012).

Supplementary Material: Boundary between noise and information applied to filtering neural network weight matrices

Max Staats,* Matthias Thamm,* and Bernd Rosenow
Institut für Theoretische Physik, Universität Leipzig, Brüderstrasse 16, 04103 Leipzig, Germany
 (Dated: June 8, 2022)

A. NEURAL NETWORK ARCHITECTURES AND TRAINING SCHEDULES

In the main text, we consider different network architectures, trained with various amounts of label noise. Tab. S1 lists the network architectures, training datasets, and accuracies achieved on each dataset. For networks trained with several different seeds, we report the average accuracy and the error of the mean. We downloaded the large pre-trained networks iv) alexnet [2] via Matlab and v) vgg19 [3] via tensorflow [4]. For the networks i)-iii), weights are initialized using the Glorot uniform distribution [5], the biases are initialized with zeros, and we standardize each image of the CIFAR-10 dataset by subtracting the mean and dividing by the standard deviation. We train networks i) and iii) for 100 epochs using mini-batch stochastic gradient descent with an initial learning rate of 0.005, an exponential learning rate schedule with decay constant 0.95, momentum of 0.95, and mini-batch size 32. For the first dense layers in the CNN, we use an L_2 regularization with strength 10^{-4} . For the discussion of accuracy improvements when shifting

Table S1. Neural network architectures and performance of trained networks. We use d to indicate a dense layer, c for a convolutional layer, p for max pooling, f for flattening, and r for response normalization layer (with a depth radius of 5, a bias of 1, $\alpha = 1$, and $\beta = 0.5$).

	network	dataset	noise	training acc	test acc
i)	3 hidden layers {d 3072, d 1024, d 512, d 512, d 10} (MLP1024)	CIFAR-10	0%	100.0%	(56.99 ± 0.11)%
			10%	100.0%	(52.10 ± 0.12)%
			20%	100.0%	(48.26 ± 0.13)%
			30%	100.0%	(44.55 ± 0.15)%
			40%	100.0%	(40.57 ± 0.11)%
			50%	100.0%	(36.69 ± 0.11)%
			60%	100.0%	(32.46 ± 0.23)%
			70%	100.0%	(27.85 ± 0.15)%
			80%	100.0%	(23.13 ± 0.19)%
			100%	100.0%	10.3%
ii)	3 hidden layer {d 3072, d 1024, d 512, d 512, d 10} (MLP1024) overfitting schedule	CIFAR-10	0%	100.0%	(55.99 ± 0.11)%
			10%	100.0%	(51.72 ± 0.10)%
			20%	100.0%	(47.77 ± 0.11)%
			30%	100.0%	(43.60 ± 0.13)%
			40%	100.0%	(38.84 ± 0.15)%
			50%	100.0%	(34.04 ± 0.14)%
			60%	100.0%	(29.01 ± 0.08)%
			70%	100.0%	(23.94 ± 0.08)%
		80%	100.0%	(19.06 ± 0.09)%	
iii)	CNN {c 300 5 × 5, p 3 × 3, r, c 150 5 × 5, p 3 × 3, r, f, d 384, d 192, d 10} (miniAlexNet) [1]	CIFAR-10	0%	100%	78.5%
			20%	100%	66.4%
			40%	100%	49.8%
			100%	100%	10.2%
iv)	alexnet [2]	ImageNet	0%		57.1%
v)	vgg19 [3]	ImageNet	0%		71.8%

* These authors contributed equally to this work.

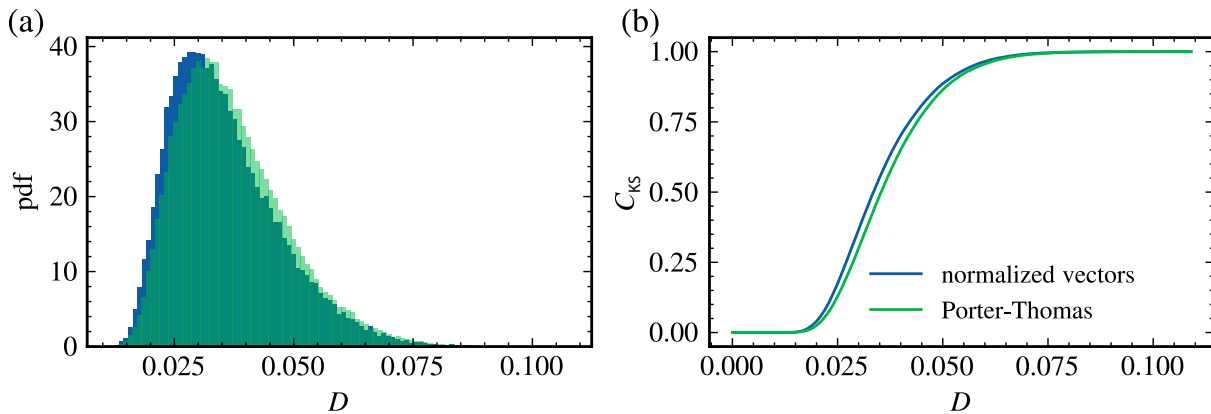


Figure S1. Comparison between Kolmogorov-Smirnov test statistics for random vectors of length 512 with i.i.d. entries (green) and for normalized vectors (blue). (a) Probability density function of the Kolmogorov-Smirnov distances Eq. (S4) obtained with Monte-Carlo sampling. (b) Cumulative distribution functions for the pdfs shown in (a). It becomes apparent that normalizing the vectors significantly changes the Kolmogorov-Smirnov test statistics even though it leaves the cumulative distribution of the vector entries unchanged.

and removing singular values we also consider an overfitting training schedule ii) with 500 epochs, with a stepwise schedule starting at a learning rate 0.001, which is then reduced it by a factor of 0.7 every 50 epochs. This ensures that we train for a large number of epochs after reaching 100% training accuracy.

B. RESHAPING OF CONVOLUTIONAL LAYER WEIGHTS

For convolutional layers, weights are 4D tensors such that we need to reshape them first to a matrix shape before computing the singular value decomposition. A weight W of shape (K, L, M, N) with $K > L > M > N$ is reshaped to a matrix \tilde{W} with sizes $(K, L \cdot M \cdot N)$ according to

$$\tilde{W}_{k,(l \cdot M \cdot N + m \cdot N + n)} = W_{k,l,m,n} \quad (\text{S1})$$

with indices counted from zero. This way, elements that are close to each other in the tensor remain close in the matrix [6].

C. FITTING MARCHENKO-PASTUR CURVES

In the main text, we fit the singular value density of DNN weight matrices to the Marchenko-Pastur (MP) distribution [7]

$$P(\nu) = \begin{cases} \frac{n/m}{\pi \sigma^2 \nu} \sqrt{(\nu_{\max}^2 - \nu^2)(\nu^2 - \nu_{\min}^2)} & \nu \in [\nu_{\min}, \nu_{\max}] \\ 0 & \text{else} \end{cases} \quad (\text{S2})$$

with $\nu_{\min} = \sigma(1 - \sqrt{m/n})$ to obtain the standard deviation of the noise term σ used in the shifting formula Eq. (3). As the spectrum additionally has singular values in the tail, the MP part is not normalized and the end of the MP region is not known a priori. We therefore first broaden the DNN spectrum using Gaussian broadening [8]

$$P(\nu) \approx \frac{1}{m} \sum_{k=1}^m \frac{1}{\sqrt{2\pi\sigma_k^2}} \exp\left(-\frac{(\nu - \nu_k)^2}{2\sigma_k^2}\right). \quad (\text{S3})$$

with $\sigma_k = (\nu_{k+a} - \nu_{k-a})/2$ and windows size $a = 15$, and then fit an adjusted MP distribution, where we use ν_{\max} and the maximum height as independent fit parameters, and infer ν_{\min} from the smallest singular values. This yields an estimate for ν_{\min} and ν_{\max} . We then fit the proper MP distribution Eq. (S2), only depending on σ , to a normalized histogram of the singular values between ν_{\min} and ν_{\max} .

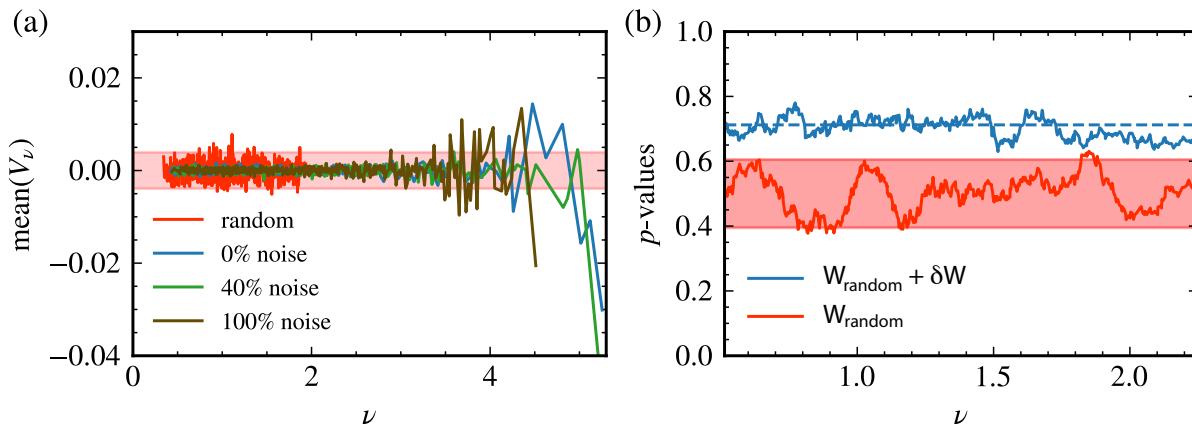


Figure S2. (a) Mean values of singular vector components for the first hidden layer of the trained MLP1024 DNN (same vectors as in Fig. 1 main text) as a function of the corresponding singular values ν . The red line shows the distribution of means for singular vectors of a random random weight matrix with i.i.d. Gaussian entries, with the corresponding 2σ region shown as transparent red stripe. We observe means much closer to zero for singular vectors of the trained weight matrix in the case of small singular values, and significantly larger means for the vectors corresponding to large singular values. (b) Kolmogorov-Smirnov p -values (with test statistics from Sec. D) for singular vectors of a 1024×512 matrix W_{random} (red) with i.i.d. Gaussian entries with zero mean and variance $1/512$; 2σ region for p -values shown in light red. When adding a matrix δW of rank ten with entries from a Gaussian distribution with the same variance but with mean -0.01 (similar to mean values observed for empirical vectors corresponding to the largest singular values in (a)), the sum $W_{\text{random}} + \delta W$ (blue) has singular vectors with significantly increased p -values, due to the requirement of orthogonality between singular vectors with large and small singular values. The p -values are averaged over neighboring singular values with a window size of 15.

D. KOLMOGOROV-SMIRNOV TEST STATISTIC FOR NORMALIZED PORTER-THOMAS VECTORS

Entries of N -dimensional singular vectors ξ_i of random matrices from the Gaussian orthogonal ensemble follow the cumulative Porter-Thomas distribution function $C_{\text{PT}}(x) = 1/2 + \text{erf}(\sqrt{N/2} x)/2$. However, their entries are not uncorrelated due to the normalization condition $\sum_i \xi_i^2 = 1$. Hence, the statistic of the usual Kolmogorov-Smirnov test which determines the p -values for uncorrelated data cannot be applied here. We obtain the statistic for normalized vectors using Monte-Carlo sampling of 50000 normalized random vectors $\xi^{(k)}$ by computing the empirical cdf for each vector $C_{\text{emp}}^{(k)}(\xi^{(k)})$ to find the corresponding Kolmogorov-Smirnov distances

$$D^{(k)} = \sup_x |C_{\text{emp}}^{(k)}(\xi^{(k)}) - C_{\text{PT}}(\xi^{(k)})|. \quad (\text{S4})$$

The cdf $C_{\text{KS}}(D)$ for the 50000 distances $\{D^{(k)}\}$ allows to determine the p -values for a given new vector ξ with deviation $D(\xi)$ as $1 - p = C_{\text{KS}}(D(\xi))$. The deviations between the usual Kolmogorov-Smirnov statistic (green) and the sampled statistic for normalized vectors (blue) are shown in Fig. S1.

E. INCREASED p -VALUES

In main text Fig. 1 we test the singular vector entries of trained weight matrices against the Porter-Thomas distribution and find that the p -values in the random part of the spectrum are significantly higher than statistically expected. We argue that this is due to the presence of a few non-random singular vectors that store the information. These vectors force the random singular vectors to have a narrower distribution around the most likely part of the Porter-Thomas distribution (normal distribution with zero mean) due to the constraint of orthogonality with the deviating singular vectors with large singular values.

For example, using the same test statistic as described in Sec. D such that random normalized vectors from the Porter-Thomas distribution have on average a p -value of 0.5, the subset of vectors with zero mean have an average p -value of 0.74. We show in Fig. S2(a) that the mean values of singular vector entries for small singular values of trained weight matrices (0% label noise blue, 40% green, 100% brown) are indeed smaller than the expected values

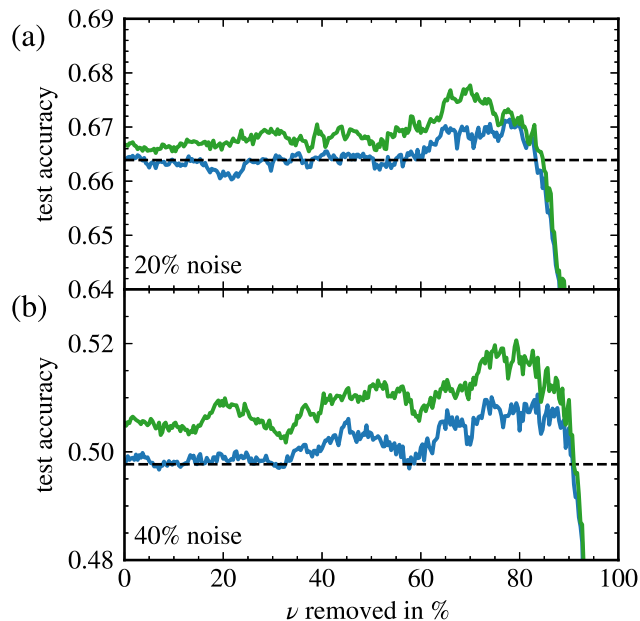


Figure S3. Dependence of the test accuracy on the removal and shifting of singular values from the weight matrix of the first convolutional layer in miniAlexNet after training with label noise. The dashed lines depict the test accuracy without removing singular values. We compare setting singular values to zero (blue) with additionally shifting the singular values (green) according to main text Eq. (3). (a) For training on CIFAR-10 with 20% label noise, and (b) for 40% label noise.

(2σ range in light red stripe) for fully random matrices (red) while the means are much larger for large singular values where the information is stored.

The increase of p -values can also be shown for a simple model, adding a low-rank matrix δW to a fully random matrix W_{random} that would have singular vectors with p -value of 0.5 on average. For this we draw a 1024×512 matrix W_{random} with Gaussian distributed i.i.d. entries with mean zero and variance $1/512$, for which the p -values of singular vectors fluctuate around 0.5 (see red curve in Fig. S2(b), with most values within the 2σ region (light red stripe)). We then draw a second 1024×512 matrix with i.i.d. Gaussian distributed entries with mean -0.01 and variance $1/512$, compute the singular value decomposition, and reconstruct the matrix by only keeping the largest 10 singular values yielding a rank 10 matrix δW . We then analyze the p -values of the singular vectors of $W_{\text{random}} + \delta W$. We find that the p -values are increased (blue line in Fig. S2(b)), with mean 0.71, which shows that in the presence of a few singular vectors with a distribution different from the random bulk, we expect the p -values in the bulk to be increased due to the enforced orthogonality to the singular vectors with a finite mean.

F. CLEANING OF A CONVOLUTIONAL LAYER

In Fig. S3 we show improvements of the test accuracy when filtering weights from convolutional layers of miniAlexNet networks (analogous to Fig. 4 in the main text), both with and without shifting of eigenvalues. The results are very similar to the behavior for dense layers described in the main text.

* These authors contributed equally to this work.

- [1] C. Zhang, S. Bengio, M. Hardt, B. Recht, and O. Vinyals, Communications of the ACM **64**, 107 (2021).
- [2] A. Krizhevsky, I. Sutskever, and G. E. Hinton, Communications of the ACM **60**, 84 (2017).
- [3] K. Simonyan and A. Zisserman, preprint arXiv:1409.1556 (2014).
- [4] M. Abadi, A. Agarwal, P. Barham, E. Brevdo, Z. Chen, C. Citro, G. S. Corrado, A. Davis, J. Dean, M. Devin, S. Ghemawat, I. Goodfellow, A. Harp, G. Irving, M. Isard, Y. Jia, R. Jozefowicz, L. Kaiser, M. Kudlur, J. Levenberg, D. Mané, R. Monga, S. Moore, D. Murray, C. Olah, M. Schuster, J. Shlens, B. Steiner, I. Sutskever, K. Talwar, P. Tucker, V. Vanhoucke,

- V. Vasudevan, F. Viégas, O. Vinyals, P. Warden, M. Wattenberg, M. Wicke, Y. Yu, and X. Zheng, “TensorFlow: Large-scale machine learning on heterogeneous systems,” (2015), software available from tensorflow.org.
- [5] Xavier Glorot and Yoshua Bengio, Proceedings of the Thirteenth International Conference on Artificial Intelligence and Statistics , 249 (2010).
- [6] Y. Yoshida and T. Miyato, preprint arXiv:1705.10941 (2017).
- [7] V. A. Marčenko and L. A. Pastur, Mathematics of the USSR-Sbornik **1**, 457 (1967).
- [8] V. Plerou, P. Gopikrishnan, B. Rosenow, L. A. N. Amaral, T. Guhr, and H. E. Stanley, Physical Review E **65**, 066126 (2002).